Journal of the American Heart Association

ORIGINAL RESEARCH

Large-Conductance Calcium-Activated Potassium Channel Opener, NS1619, Protects Against Mesenteric Artery Remodeling Induced by Agonistic Autoantibodies Against the Angiotensin II Type 1 Receptor

Meili Wang, PhD; Xiaochen Yin, MD; Shuanglei Li, MD; Xi Zhang, MD; Ming Yi, MD; Chunyu He, MD; Xiaoyue Li, MD; Wei Wang, PhD; Suli Zhang, PhD; Huirong Liu, MD, PhD

BACKGROUND: Agonistic autoantibodies against the angiotensin II type 1 receptor (AT1-AAs) extensively exist in patients with hypertensive diseases and have been demonstrated to play crucial roles in the pathophysiological process of vascular remodeling. However, the treatment options are limited. The large-conductance calcium-activated potassium (BK) channel is a critical regulator and potential therapeutic target of vascular tone and architecture. We have previously observed that AT1-AAs have an inhibitory effect on BK channels. However, whether BK channel dysfunction is involved in AT1-AAs-induced vascular remodeling and the therapeutic effect of BK channel opener is unclear.

METHODS AND RESULTS: In our study, mesenteric arteries from AT1-AAs-positive rats exhibited increased wall thickness, narrowing of the arteriolar lumen, and increased collagen accumulation. Patch clamp test results showed that the voltage sensitivity of BK channel declined in mesenteric arteriolar smooth muscle cells from AT1-AAs-positive rats. Experiments with freshly isolated mesenteric arteriolar smooth muscle cells showed that AT1-AAs reduced the opening probability, open levels, open dwell time, and calcium sensitivity of BK channel. Experiments with HEK293T cells transfected with GFP-ZERO-BK α-subunit plasmids suggested a BK channel α-subunit-dependent mechanism. BK channel α-subunit deficient, namely *KCNMA1*$^{-/-}$ rats showed a phenotype of mesenteric artery remodeling. The administration of NS1619, a specific BK channel opener targeting the α-subunit, reversed the phenotypic transition and migration induced by AT1-AAs in cultured mesenteric arteriolar smooth muscle cells. Finally, perfusion of NS1619 significantly relieved the pathological effects induced by AT1-AAs in vivo.

CONCLUSIONS: In summary, we provide compelling evidence that BK channel α-subunit dysfunction mediates AT1-AAs-induced mesenteric artery remodeling. Preservation of BK channel activity may serve as a potential strategy for the treatment of AT1-AAs-induced maladaptive resistance artery remodeling.

Key Words: angiotensin II type 1 receptor ■ autoantibody ■ BK channel ■ NS1619 ■ vascular remodeling

Remodeling of the resistance arteries is one of the earliest detectable parameters that predict subsequent life-threatening cardiovascular events.[1,2] It is found in almost all subjects with hypertension, with a reduction in the lumen and external diameters but without increase in its media cross-section. It contributes to increased peripheral vascular resistance and may participate in the development and complications

Correspondence to: Huirong Liu, Department of Physiology and Pathophysiology, School of Basic Medical Sciences Capital Medical University, No.10 Xitoutiao, You An Men, Beijing 100069, China. E-mail: liuhr2000@126.com and Suli Zhang, Department of Physiology and Pathophysiology, School of Basic Medical Sciences Capital Medical University, No.10 Xitoutiao, You An Men, Beijing 100069, China. E-mail: sueney716@126.com

Supplemental Material for this article is available at https://www.ahajournals.org/doi/suppl/10.1161/JAHA.121.024046.

For Sources of Funding and Disclosures, see page 11.

JAHA is available at: www.ahajournals.org/journal/jaha

CLINICAL PERSPECTIVE

What Is New?

- Autoantibodies against the angiotensin II type 1 receptor impair large-conductance calcium-activated potassium channel function and cause inward eutrophic mesenteric artery remodeling.
- Pharmacologic large-conductance calcium-activated potassium channel activation protects from deleterious effects of autoantibodies against the angiotensin II type 1 receptor in vitro and in vivo.

What Are the Clinical Implications?

- Therapies that enhance large-conductance calcium-activated potassium channel activity may provide cardiovascular protection in patients with hypertension and autoantibodies against the angiotensin II type 1 receptor.

Nonstandard Acronyms and Abbreviations

AT1-AAs	autoantibodies against the angiotensin II type 1 receptor
AT_1R	angiotensin II type 1 receptor
BK	large-conductance calcium-activated potassium channel
MA	mesenteric artery
MASMC	mesenteric arteriolar smooth muscle cell
SD	Sprague-Dawley
VSMC	vascular smooth muscle cell

of hypertension, including myocardial ischemia, stroke, and renal failure.[3] In fact, the high degree of artery remodeling predicts worse prognosis for subjects with hypertension.[4] The pathophysiological mechanisms responsible for resistance artery remodeling, however, are complex and incompletely understood.

Excessive activation of the angiotensin II type 1 receptor (AT_1R) induces resistance artery remodeling and the selective antagonism of AT_1R improves it.[4] Intriguingly, the effect of AT_1R blockers is often superior to that of angiotensin converting enzyme inhibitors,[5,6] suggesting that apart from angiotensin II, other factors may be involved in the activation of AT_1R. However, how it occurs is not fully understood. Over the past decades, studies have shown that autoantibodies against the AT_1R (AT1-AAs) were involved in the excessive activation of this receptor. AT1-AAs exhibit an agonist-like effect via the binding and activation of AT_1R. They trigger uncontrolled signaling cascades and thus produce pathologies.[7,8] Since their discovery, AT1-AAs have been closely related with hypertensive diseases.[9–11] Moreover, AT1-AAs have proven to be a causative player in small arteries remodeling.[12,13] AT1-AAs regulate physiological processes ranging from collagen production to angiogenesis modulation.[14,15] Currently, the treatment options for AT1-AAs-induced vascular diseases are limited. In addition, AT_1R blockers are strictly prohibited under certain circumstances (such as pregnancy). Therefore, although the role of AT1-AAs in driving resistance artery remodeling is well defined, it is less clear how to eliminate the harmful effects.

The inward eutrophic remodeling of arterioles is closely associated with augmented active tone induced by prolonged vasoconstriction.[3] In line with this, current evidence of the effect of ion channels on myogenic tone points to their important role in the regulation of the development of vascular remodeling. The large-conductance calcium-activated potassium (BK) channel is an important potassium channel that is involved in negative feedback regulation of the vascular smooth muscle cell (VSMC) membrane potential and myogenic tone.[16] That is, activation of BK channels leads to the efflux of K^+ and causes VSMC hyperpolarization, which in turn causes L-type Ca^{2+} channel closure and subsequent vasodilation.[17,18] Particularly, BK channel deficiency promotes mesenteric artery (MA) fibrosis and remodeling.[19] In a previous study, we have shown that AT1-AAs have an inhibitory effect on BK channels,[20] indicating a possible close relationship between impaired BK channel function and AT1-AAs-induced vascular damage. However, there is still no direct evidence. We, therefore, proceeded to investigate it and assess strategies for restoring BK channel function using NS1619, a specific BK channel opener, in this process.

METHODS

The data that support the findings of this study are available from the corresponding author upon reasonable request. A complete description of Methods is provided in Data S1.

Animal Experiments

All experimental procedures were approved by the Institutional Animal Care and Use Committee and Ethics Committee of Capital Medical University (Beijing, China) and were in strict accordance with the recommendation in the *Guide for the Care and Use of Laboratory Animals* of the National Institutes of Health. Healthy male Sprague-Dawley (SD) rats aged 8 weeks (140–160 g) were obtained from the Animal Center of Capital Medical University and housed under a 12:12-h dark-light cycle in standard conditions of humidity and

room temperature. Before immunization, blood collection from the tip of the tail, or the subcutaneous implantation of osmotic mini-pumps, rats were anesthetized with an intraperitoneal injection of 40 mg/kg sodium pentobarbital. At the end of the experiment, the rats were euthanized with an intraperitoneal injection of 100 mg/kg sodium pentobarbital. Active immunization was carried out as previously described.[13] Briefly, male SD rats aged 8 weeks were randomly divided into 2 groups: the Freund's adjuvant emulsified AT_1R-EC_{II} (epitope peptide of the extracellular second loop of the AT1R) peptide-immunized group and the Freund's adjuvant emulsified saline-treated vehicle group. The immunization was repeated by subcutaneous injection with AT_1R-EC_{II} every 2 weeks. The blood pressure was measured at 2-week intervals with the standard tail-cuff technique (Softron, Japan) using the Powerlab system. Blood samples were collected every 2 weeks before immunization. The relative amounts of AT1-AAs in sera were determined by ELISA as previously described.[13] The preparation of immunoglobulin G from serum was performed as previously described.[13] For the in vivo experiments involving NS1619 treatment, saline-treated or peptide fragments-immunized rats were divided into 4 groups at the end of the fourth week of immunization. Rats were infused with NS1619 (20 μg/kg per day) for 6 weeks via implanted osmotic mini-pumps. $AT_1R^{-/-}$ and *KCNMA1*$^{-/-}$ rats were constructed by Nanjing Biomedical Research Institute of Nanjing University.

Statistical Analysis

Statistical analysis was performed by GraphPad Prism (GraphPad Software, Inc., San Diego, CA, USA). Data are expressed as the means±SEM. Differences between the 2 groups were analyzed by Student's *t* test. Differences between multiple groups were analyzed by 2-way ANOVA followed by the Bonferroni post hoc test. $P<0.05$ was recognized as statistically significant.

RESULTS

AT1-AAs-Positive Rats Exhibited MA Remodeling

To validate the pathological effects of AT1-AAs on vascular remodeling, we first established an AT1-AAs-positive rat model by active immunization. Serum levels of AT1-AAs were determined by ELISA. The results showed that the antibodies appeared 2 weeks after the first immunization and increased gradually with the duration of immunization (Figure S1A). The levels of serum AT1-AAs peaked at the 6th week and were maintained until the end of the experiment, suggesting that the AT1-AAs-positive rat model was successfully established. In the control group, no AT1-AAs were detected throughout the whole process.

Heart rates and blood pressure were monitored in conscious rats by the tail-cuff method. The heart rate showed no significant difference between the 2 groups (Figure S1B). Compared with the control group, the AT1-AAs-positive rats showed a marked elevation in the systolic blood pressure at the 4th week after the first immunization. However, it was similar to that observed in the control rats during and after the 6th week, and even lower at the 12th week (Figure S1C). Changes in the diastolic blood pressure were consistent with systolic blood pressure (Figure S1D).

At the end of the 10th week of immunization, MA sections were used for morphological examination. Hematoxylin-eosin staining showed that the AT1-AAs-positive MAs exhibited greater media wall thickness and reduced lumen and external diameters compared to the control MAs. Whereas, there was no significant change in the media cross-sectional area of MAs between the 2 groups (Figure 1A). Masson's trichrome staining showed increased collagen accumulation in the AT1-AAs-positive MAs, especially in the adventitial and medial layers (Figure 1B). These results demonstrated that the long-term existence of AT1-AAs induced MA remodeling.

BK Channel Activity Was Inhibited in the MASMCs from AT1-AAs-Positive Rats

We next investigated the effects of AT1-AAs on BK channel during the process of MAs remodeling. First, we verified the types of the splicing variants of the BK channel α-subunit that were present in MAs. Total RNA of MAs from normal SD rats was extracted and reverse-transcribed. Then, the cDNA was amplified by PCR using the constructed BK-trans primers (Figure S2A). Electrophoretic analysis showed that most of the amplified products were 230 bp in size (Figure S2B), suggesting that most of the BK channel α-subunits in the MAs were of the ZERO type. Therefore, in the follow-up experiments, we mainly focused on the ZERO-BK α-subunit isoform.

We first detected the expression level of BK channels. As shown in Figure S3, there was no significant change in the protein level of BK α. To explore the effects of AT1-AAs on BK channel function, we performed patch clamp experiments. Mesenteric arteriolar smooth muscle cells (MASMCs) were freshly isolated from control and AT1-AAs-positive rats in the 8th week after the first immunization. In on-cell mode, step voltage clamping was used to detect the electrical activity of the BK channel (Figure 2A). Compared with that in the control group, the voltage sensitivity of the BK channel was decreased in the MASMCs from the AT1-AAs-positive rats (Figure 2B). This result

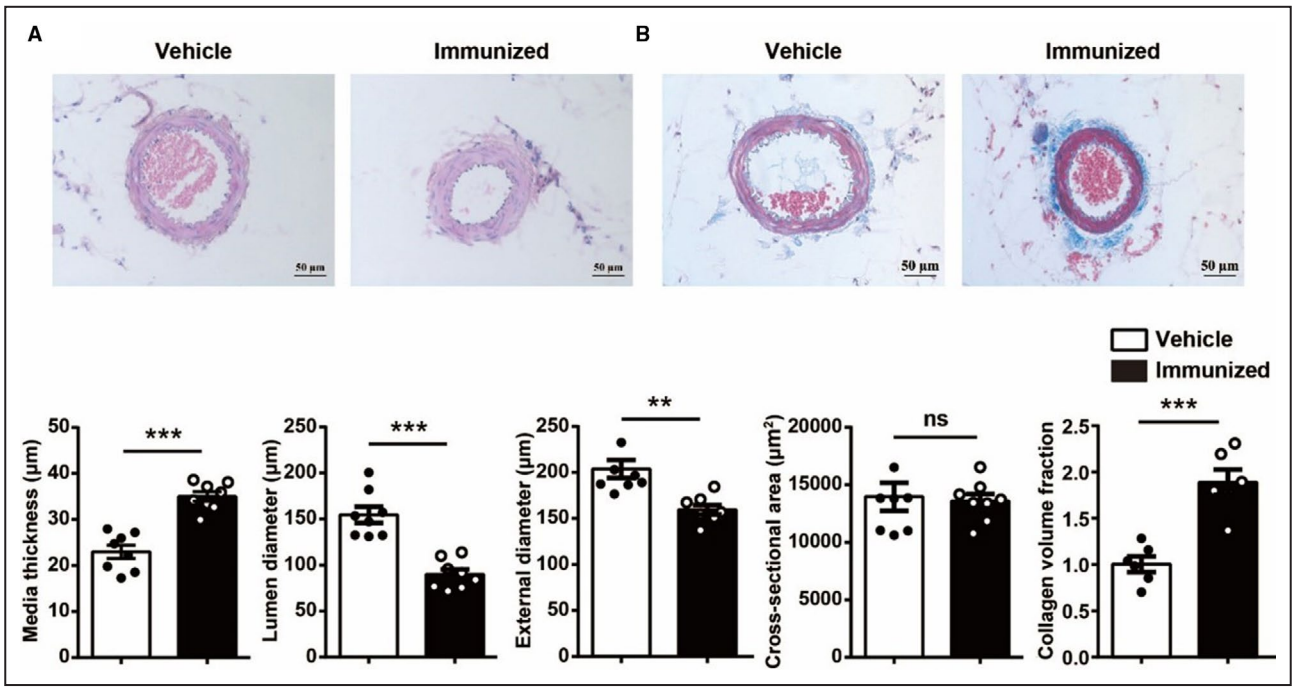

Figure 1. MAs from AT1-AAs-positive rats exhibited remarkable vascular remodeling and perivascular fibrosis.
A, Representative microscopic images of hematoxylin-eosin stained MA sections and statistical diagrams of the media wall thickness, lumen diameter, external diameter, and CSA. **B**, Masson's trichrome staining of MA sections to highlight perivascular fibrosis (blue-stained connective tissue). Data were analyzed by the Student *t* test. n=6–8 rats per group. ***P*<0.01, ****P*<0.001. AT1-AAs indicates agonistic autoantibodies against the angiotensin II type 1 receptor; CSA, cross-sectional area; MA, mesenteric artery; and ns, not significant.

suggested that AT1-AAs had an inhibitory effect on BK channel activity in the early stage of MA remodeling.

AT1-AAs Inhibited the Electrical Activity of the BK Channel in MASMCs in vitro

To further validate the direct inhibitory effects of AT1-AAs on BK channels, we performed an in vitro experiment. AT1-AAs were harvested from the sera of AT1-AAs-positive rats, purified by an IgG purification column and centrifugally concentrated by ultrafiltration. The purity and activity of the purified AT1-AAs were validated by Coomassie blue staining and neonatal rat cardiomyocyte beating number experiments, respectively (Figure S4). MASMCs from normal SD rats were freshly isolated and subjected to patch clamp

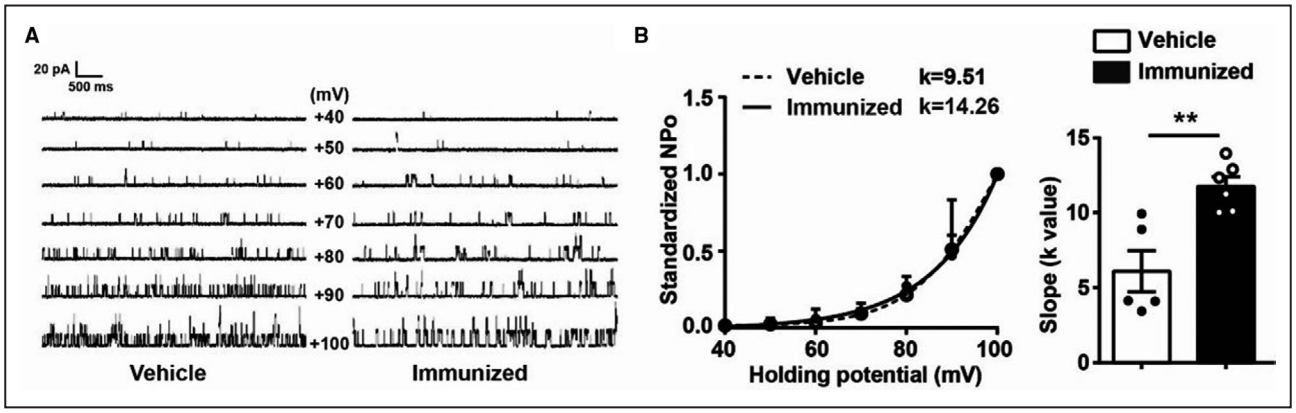

Figure 2. BK channel function was detected in MASMCs from rats of the control and immunized groups.
A, The electrical activity of the BK channel was recorded in MASMCs isolated from rats of the control and immunized groups. **B**, The opening probability of the BK channel with increasing voltage stimulation. The Boltzmann equation was used for fitting and standardization. The slope (k value) of the fitted Boltzmann equation was negatively correlated with the voltage sensitivity of the BK channel. Data were analyzed by Student's *t* test. n=5 or 6 rats per group. ***P*<0.01. BK channel indicates large-conductance calcium-activated potassium channel; and MASMC, mesenteric arteriolar smooth muscle cell.

experiments. In on-cell mode, step voltage clamping was used to detect the electrical activity of the BK channel (Figure 3A). The results showed that after AT1-AAs treatment, the opening probability (Figure 3B) and the opening level at the same time point (Figure 3C) of the BK channel decreased significantly after AT1-AAs treatment. Moreover, the short opening time (constant τ 1) was obviously increased, whereas the long opening time (constant τ 2) was significantly decreased (Figure 3D), indicating that the overall opening time of the BK channel was shortened. These results suggested that AT1-AAs inhibited the opening capability of the BK channel at the same voltage.

We next explored whether AT1-AAs had an effect on the calcium sensitivity of the BK channel. As shown in Figure 3E and 3F, after 10 min of AT1-AAs treatment, the opening probability of the BK channel did not increase with the increasing concentrations of intracellular Ca^{2+}, indicating that the calcium sensitivity of the BK channel was almost abolished. This result indicated that AT1-AAs inhibited the calcium sensitivity of the BK channel in MASMCs.

$AT_1R^{-/-}$ rats were adopted to elucidate the involvement of AT_1R in the inhibitory effects of AT1-AAs on BK channels. MASMCs from $AT_1R^{-/-}$ rats were freshly isolated and subjected to patch clamp experiments. In on-cell mode, step voltage clamping was used to detect the activity of the BK channel (Figure S5A). The results showed that, unlike that in MASMCs from normal SD rats, the opening probability of the BK channel in MASMCs from $AT_1R^{-/-}$ rats was not significantly changed after 10 min of AT1-AAs treatment (Figure S5B), suggesting the AT_1R dependence of the inhibition of AT1-AAs on BK channels.

As an endogenous and natural ligand of AT_1R, angiotensin II has been reported to inhibit the BK channel current.[21] We then compared the differences in the inhibitory effects of angiotensin II and AT1-AAs. In on-cell mode, the electrical activity of the BK channel was recorded after angiotensin II or AT1-AAs treatment. The results showed that after 5 min of treatment, both angiotensin II and AT1-AAs inhibited the opening probability of the BK channel. However, unlike the transient effect of angiotensin II, AT1-AAs inhibited the opening probability of the BK channel even after 15 min (Figure S6). These results suggested that, compared to angiotensin II, AT1-AAs had a sustained inhibitory effect on the BK channel.

The Inhibitory Effect of AT1-AAs on BK Channels was BK Channel α-Subunit-Dependent

The α-subunit is the functional subunit of BK channel. To investigate the involvement of α-subunit in the inhibitory effect of AT1-AAs, we transfected HEK293T cells with GFP-ZERO-BK α-subunit plasmids (Figure S7A). Patch clamp experiments were performed in cells that did or did not express green fluorescence, which was observed under a fluorescence microscope. As shown in Figure S7B, the BK channel current can be detected in cells expressing green fluorescence, while it cannot be detected in cells that did not express green fluorescence. Then, we detected the electric activity of BK channels in cells successfully transfected with GFP-ZERO-BK α-subunit plasmids (Figure 4A). The results showed that the opening probability (Figure 4B) and the open level at the same time point (Figure 4C) were significantly reduced. These results suggested that in the absence of auxiliary β-subunit and γ-subunit, AT1-AAs still inhibited the electrical activity of BK channel. The inhibitory effects of AT1-AAs on BK channels were mainly α-subunit-dependent.

KCNMA1$^{-/-}$ Rats Exhibited MA Remodeling

To confirm the role of BK channel α-subunit in resistance artery remodeling, we generated *KCNMA1* knock-out rats. The *KCNMA1* gene was interrupted by deletions at exon 4 and exon 5 and frame shift mutation from exon 6 (Figure S8A). Interruption of the gene was visualized by PCR on genomic DNA from the tail tissue (Figure S8B). There was no significant difference in the heart rate between the wild type and *KCNMA1*$^{-/-}$ rats (Figure S8C). However, compared with the wild type group, the *KCNMA1*$^{-/-}$ rats showed a marked decrease in the systolic blood pressure and diastolic blood pressure (Figure S8D and S8E). Morphometric analysis showed increased media wall thickness, decreased lumen/external diameters in MAs from *KCNMA1*$^{-/-}$ rats. In addition, Masson's trichrome staining showed a significant increase in the collagen deposition, especially in the medial layers and in the adventitia (Figure 5). These results suggested that *KCNMA1*$^{-/-}$ rats exhibited similar MA remodeling as observed in AT1-AAs-positive rats.

BK Channel Activation with NS1619 Reversed AT1-AAs-Induced Phenotypic Transition of MASMCs in vitro

We investigated whether BK channel dysfunction plays a causal role in the pathogenesis of MA remodeling in response to AT1-AAs. NS1619 is a synthetic benzimidazole derivative hyperpolarizing the VSMC membrane via activation of the BK channel α-subunit. First, we validated the effects of NS1619 on AT1-AAs-induced BK channel dysfunction. After NS1619 pretreatment, the inhibitory effect of AT1-AAs on BK channels was completely reversed. That is, the opening probability of the BK channel was restored to the normal level (Figure S9). Then we isolated and cultured

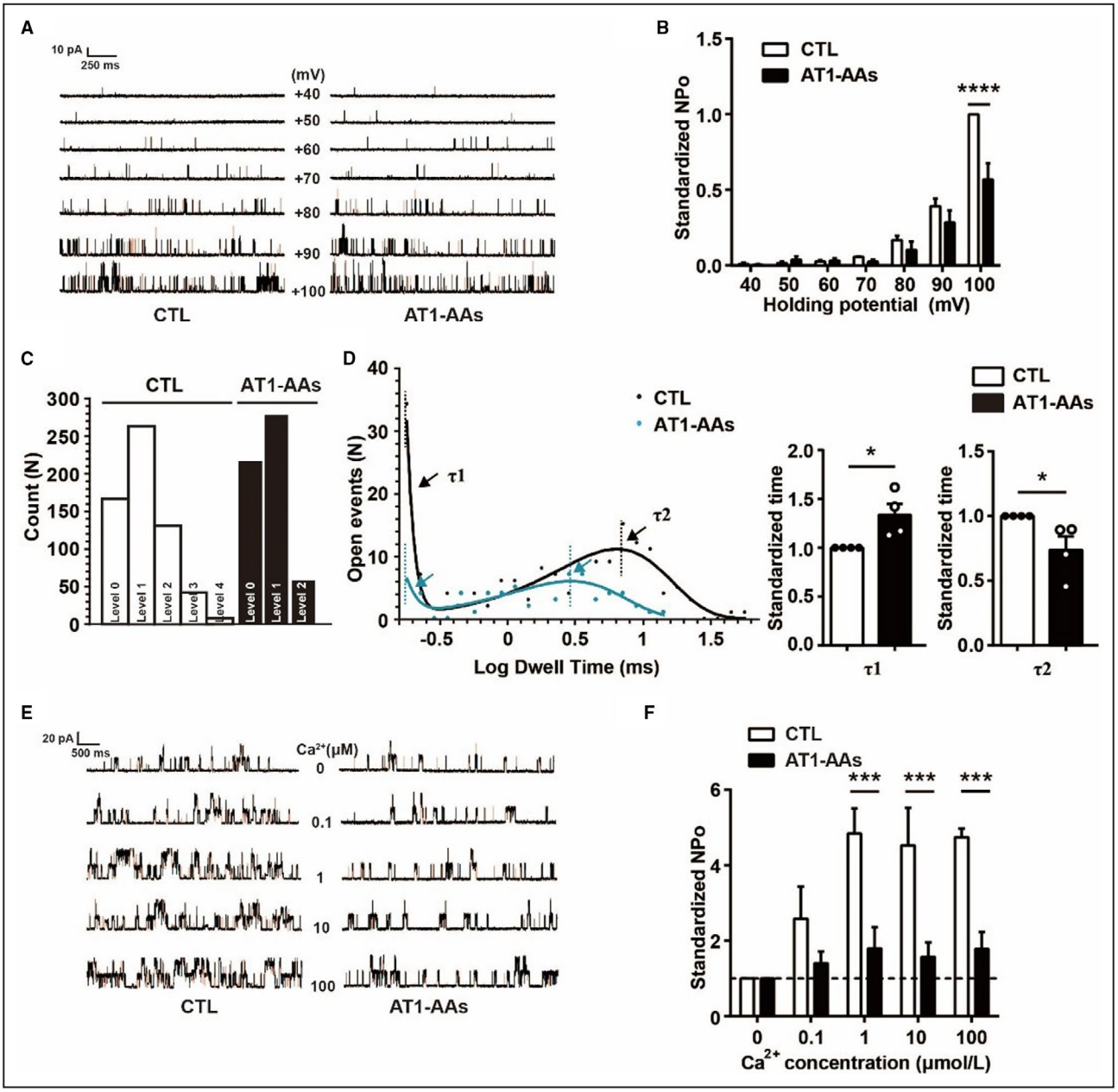

Figure 3. BK channel function was detected in MASMCs in response to AT1-AAs.
A, The electrical activity of the BK channel was recorded in MASMCs with or without AT1-AAs (0.1 μM) treatment. **B**, The opening probability of the BK channel with increasing voltage stimulation in MASMCs with or without AT1-AAs (0.1 μM) treatment. **C**, Open levels of BK channels with or without AT1-AAs (0.1 μM) treatment. **D**, An exponential distribution function in logarithmic form was used to fit the continuously changing average opening time of the BK channel. Two states (constant τ 1 and constant τ 2) in the opening of BK channel were obtained. **E**, The electrical activity of the BK channel at the indicated concentration of Ca^{2+} was recorded. **F**, The opening probability of BK channels with increasing Ca^{2+} stimulation in MASMCs with or without AT1-AAs (0.1 μM) treatment. Data were from 4–6 independent experiments and presented as the means±SEM. The Student *t* test was used. **P*<0.05, ****P*<0.001, *****P*<0.0001. AT1-AAs indicates agonistic autoantibodies against the angiotensin II type 1 receptor; BK, large-conductance calcium-activated potassium channel; CTL, control; and MASMC, mesenteric arteriolar smooth muscle cell.

MASMCs (Figure S10) and the effect of NS1619 was evaluated. NS1619 didn't change the expression of BK α (Figure S11). As shown in Figure 6A, AT1-AAs downregulated the expression of contractile proteins α-SMA, Calponin and MYH11, and these effects were attenuated by pretreatment with NS1619. The migration of VSMCs from arterial media to intima is an important event in the development of vascular remodeling.

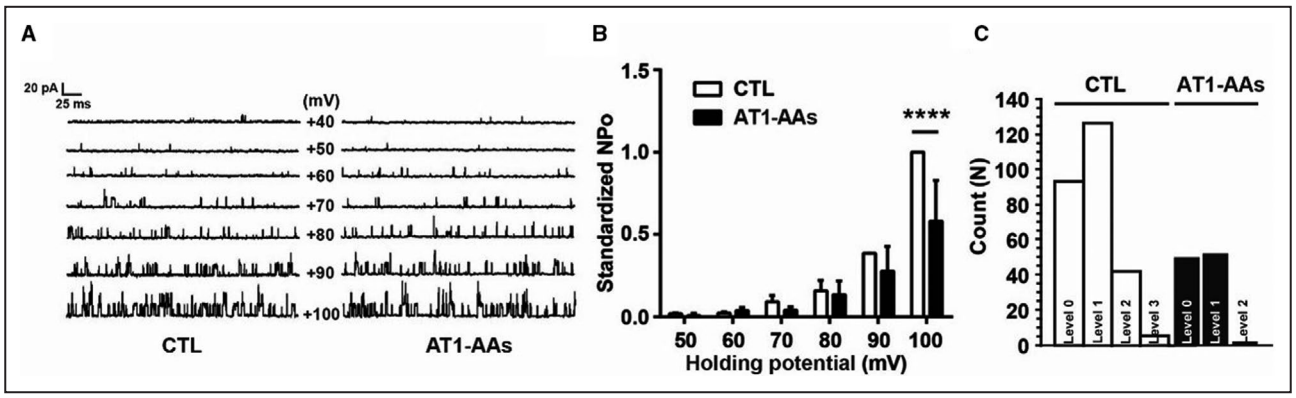

Figure 4. Detection of BK channel function in HEK293T cells transfected with ZERO-BK α-subunit plasmids.
A, The electrical activity of the BK channel was recorded in HEK293T cells successfully transfected with the ZERO-BK α-subunit plasmids. **B**, The opening probability of the BK channel with increasing voltage stimulation with or without AT1-AAs (0.1 μM) treatment. **C**, Open levels of BK channels with or without AT1-AAs (0.1 μM) treatment. The data were from 3 independent experiments and presented as the means±SEM. The Student *t* test was used. ****P<0.0001. AT1-AAs indicates agonistic autoantibodies against the angiotensin II type 1 receptor; BK, large-conductance calcium-activated potassium channel; CTL, control; and MASMC, mesenteric arteriolar smooth muscle cell.

To determine the role of BK channel dysfunction in AT1-AAs-induced VSMCs migration, MASMCs were treated with AT1-AAs with or without the pretreatment of NS1619. The scratch-wound assay revealed that AT1-AAs induced strong migration in MASMCs. The mean migration distance was longer than that of the control group and pretreatment with NS1619 significantly abolished the stimulative effect of AT1-AAs on MASMCs migration (Figure 6B).

BK Channel Activation with NS1619 Reversed AT1-AAs-Induced MA Remodeling in vivo

To support the findings, we determined the effects of NS1619 on vascular remodeling in response to AT1-AAs in vivo. The AT1-AAs-positive rats were infused with NS1619 each day by osmotic mini-pumps, starting at the end of the 4nd week of immunization until

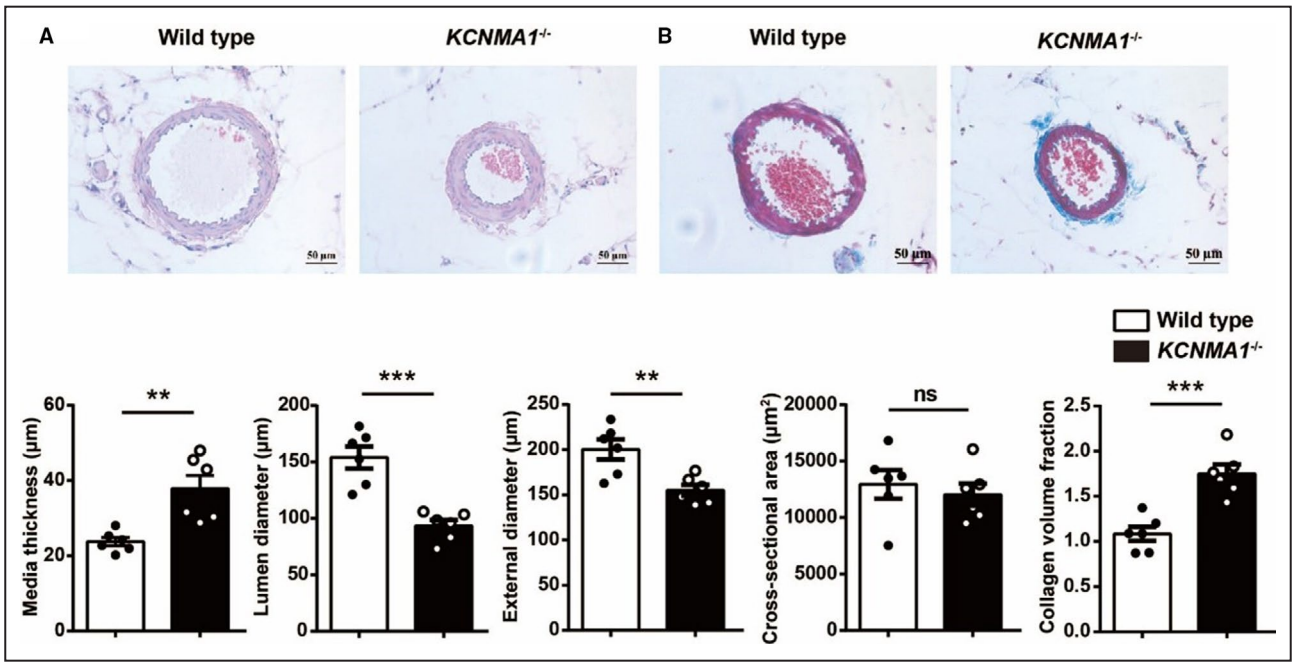

Figure 5. MAs from *KCNMA1*$^{-/-}$ rats exhibited remarkable vascular remodeling and perivascular fibrosis.
A, Representative microscopic images of hematoxylin-eosin stained MA sections and statistical diagrams of the media wall thickness, lumen diameter, external diameter and CSA. **B**, Masson's trichrome staining of MA sections to highlight perivascular fibrosis (blue-stained connective tissue). Data were analyzed by the Student *t* test. n=6 rats per group. **P<0.01, ***P<0.001. CSA indicates cross-sectional area; MA, mesenteric artery; and ns, not significant.

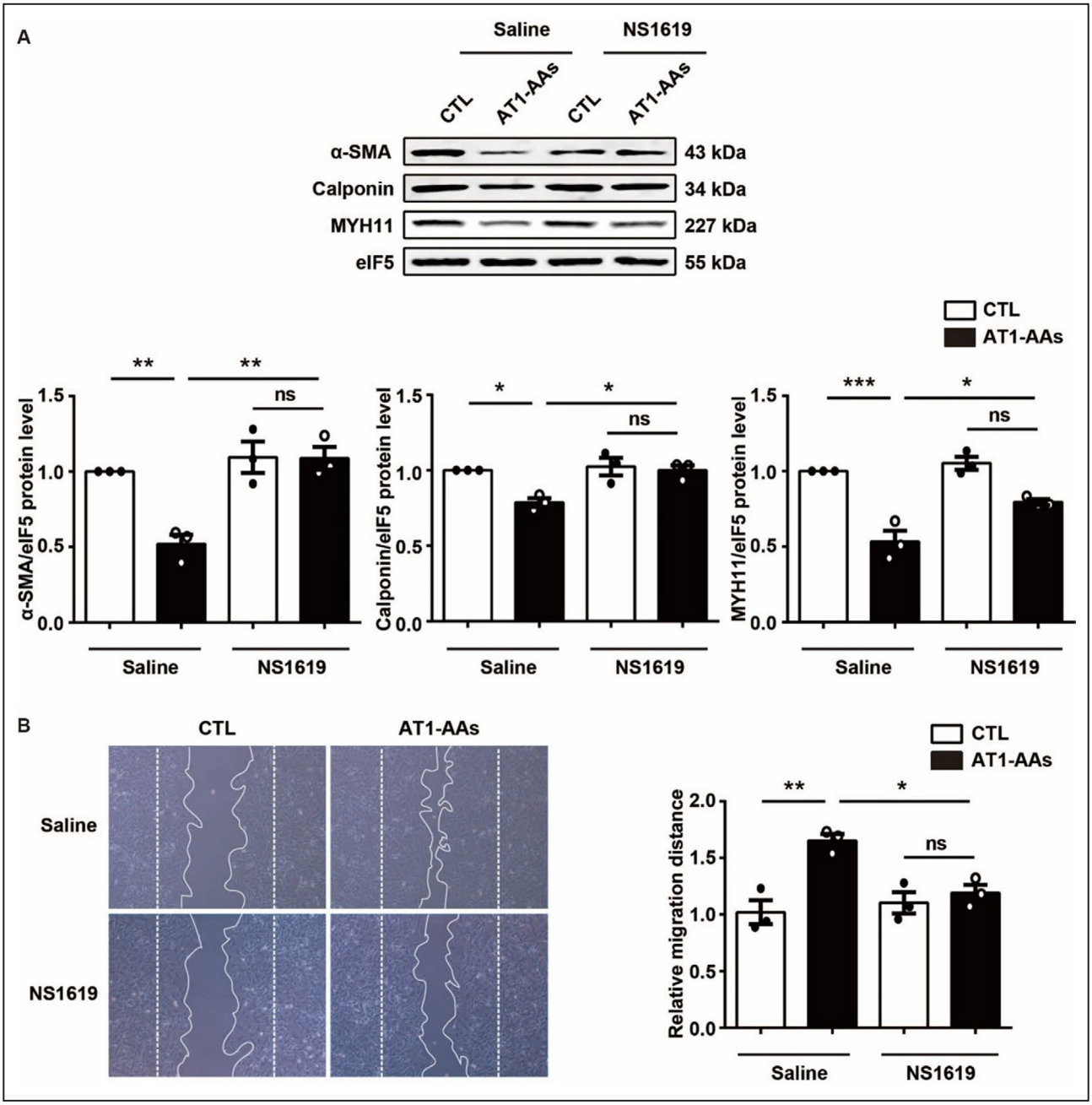

Figure 6. NS1619 pretreatment reversed the phenotypic transition and migration of MASMCs induced by AT1-AAs in vitro. **A**, Representative images and statistical diagrams of α-SMA, calponin, and MYH11 expression. MASMCs were pretreated with NS1619 (4 μM, 30 min) and then incubated with AT1-AAs (0.1 μM) for 48 hours. Cell lysates were prepared and subjected to Western blotting analysis. The data were from 3 independent experiments and presented as the means±SEM. **B**, Representative images of cell migration 24 hours after scratching. Confluent MASMC monolayers were scratch wounded 48 hours after AT1-AAs (0.1 μM) treatment. Cells were pretreated with NS1619 (4 μM, 30 min) or not. The cells were maintained in culture for an additional 24 hours before imaging (dotted line indicates wound edge). The mean distance migrated by the MASMCs was quantified (average of 4 independent microscope fields for 3 independent experiments each). Data were analyzed by 2-way ANOVA followed by the Bonferroni post hoc test. **P*<0.05, ***P*<0.01, ****P*<0.001. α-SMA indicates alpha-smooth muscle actin; AT1-AAs, agonistic autoantibodies against the angiotensin II type 1 receptor; CTL, control; MASMC, mesenteric arteriolar smooth muscle cell; and ns, not significant.

the 10th week. There was no significant change in blood pressure among the groups (Figure S12). After 6 weeks, changes in the media wall thickness, lumen/external diameters and levels of collagen deposition were significantly rescued in the NS1619-infused rats (Figure 7). These findings demonstrated that preservation of BK channel activity attenuated AT1-AAs-induced MA remodeling.

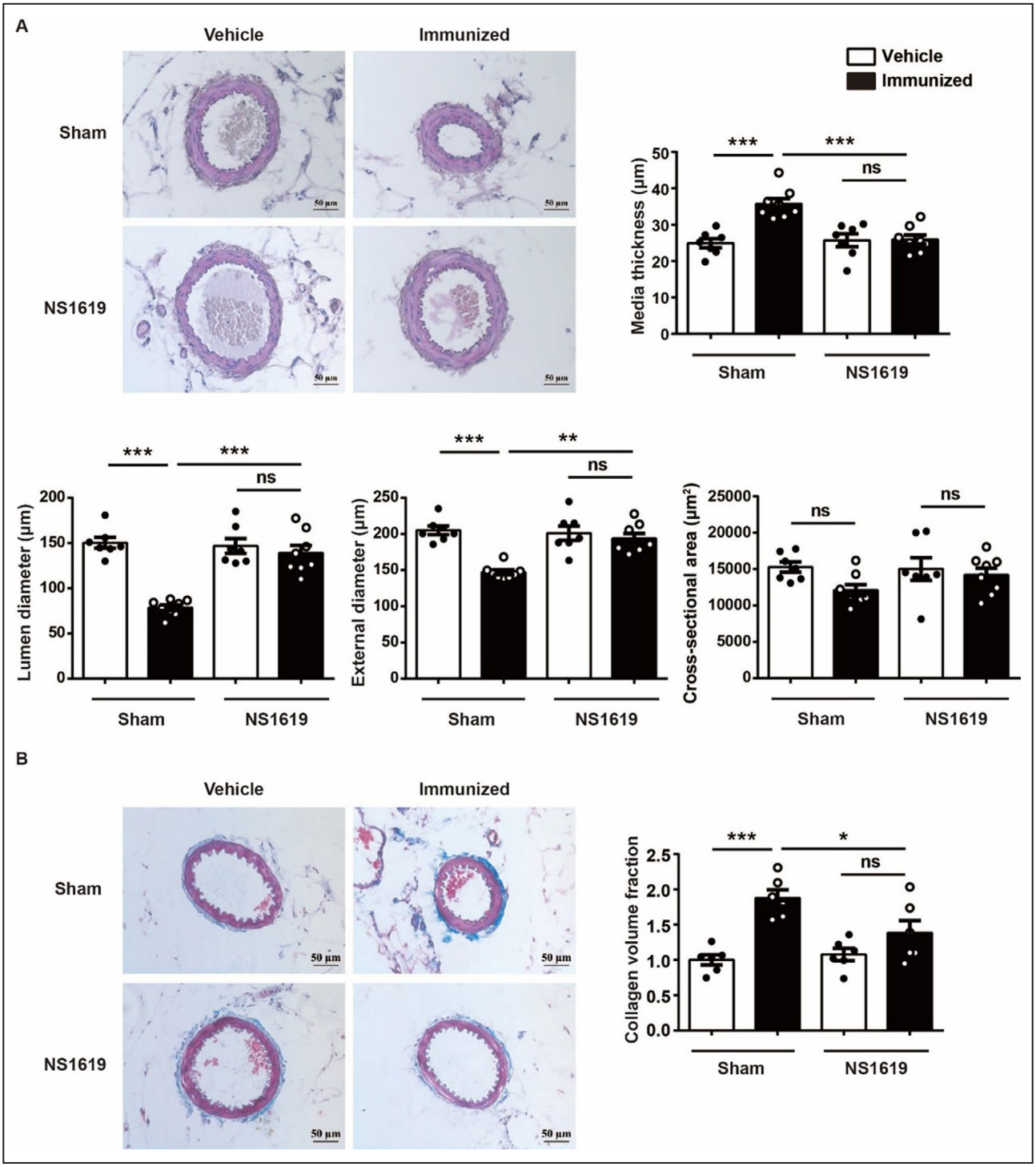

Figure 7. NS1619 perfusion reversed the remodeling and perivascular fibrosis of MAs induced by AT1-AAs in vivo.
A, Representative microscopic images of hematoxylin-eosin stained MA sections and statistical diagrams of the media wall thickness, lumen diameter, external diameter, and CSA. **B**, Masson's trichrome staining of MA sections to highlight perivascular fibrosis (blue-stained connective tissue). Rats were infused with NS1619 (20 μg/kg/day) via an osmotic mini-pump for 6 weeks. Data were analyzed by 2-way ANOVA followed by the Bonferroni post hoc test. n=6–8 rats per group. **P*<0.05, ***P*<0.01, ****P*<0.001. CSA indicates cross-sectional area; MA, mesenteric artery; and ns, not significant.

DISCUSSION

Maladaptive inward eutrophic remodeling of arteries has been shown to be a predictor of cardiovascular events.[2,22] Specifically, resistance artery remodeling is one of the fundamental pathological processes in patients with cardiovascular diseases, ultimately leading to chronic hypoxia of local organs. Chronic

vasoconstriction was suggested to be the initiator for eutrophic remodeling.[23] As an important determinant of vascular tone, BK channel deficiency contributes to resistance artery remodeling. Our study demonstrated for the first time that long-term exposure to AT1-AAs in the body causes inward eutrophic remodeling of MAs through impairment of BK channel activity. Most importantly, we confirmed the therapeutic effects of NS1619, which might be an effective therapy in clinic.

Eutrophic remodeling of the resistance arteries is characterized by reductions in the lumen and external diameters with normal cross-sectional area. It is associated with increased arterial collagen deposition and elastin fragmentation, which significantly contributes to arterial stiffness. Extracellular matrix proteins, especially collagens and fibronectin, accumulate in the media and contribute to structural and functional alterations during resistance artery remodeling. In our study, long-term exposure to AT1-AAs caused a marked increase in the mesenteric resistance artery medial thickness and extracellular matrix protein deposition, which are typical features of inward eutrophic MA remodeling.

During the process of immunization, blood pressure began increasing at the 2nd week and peaked at the 4th week, which reflects a vasopressor effect of AT1-AAs. After that, blood pressure declined and became even lower than that of the control rats. Our previous research and studies of other groups have shown similar results.[12,13] It might be because the decreased cardiac function by the long-existing AT1-AAs, which has been confirmed previously.[24] Another possibility is, blood pressure in the immunized group was adjusted by other antihypertensive mechanisms.

In theory, strategies targeting AT1-AAs mainly include elimination of this autoantibody from the patients' circulation or in vivo treatment with AT_1R blockers. For the elimination of AT1-AAs, technologies are under development and difficult to be extensively used.[25] On the other hand, an AT_1R blocker therapy is not appropriate in conditions such as pregnant women since the treatment is leading to severe maldevelopment of the kidney in the fetus.[26,27] Therefore, there is an urgent need for a safer and more effective method blocking AT1-AAs-induced vascular remodeling. BK channel is the most dense and important calcium-activated potassium channel on VSMCs. Its opening can mediate K^+ outflow and hyperpolarize the cell membrane, thus inhibiting excessive Ca^{2+} influx and preventing sustained vascular contraction.[17] In the blood vessels, BK channels have been regarded as an important determinant of blood pressure, heart rate and vascular function/structure. Numerous animal studies have shown that BK channel deficiency contributes to increased vascular tone and blood pressure regulation.[28–31] Particularly, long-term changes in BK channel voltage and calcium sensitivity can lead to vascular wall thickening, fibrosis enhancement and vascular remodeling.[19] Our recent findings showed that the electrical activity of BK channels in the MASMCs from AT1-AAs-positive pregnant mice was decreased.[20] In this study, we validated this effect with an active immunized rat model. In the AT1-AAs-positive group, the expression level of BK channel was unchanged while the voltage sensitivity of the BK channel was significantly decreased. These findings suggested the decreased BK electrical activity rather than expression change in this process. To further investigate the specific inhibitory effects of AT1-AAs on BK channels, we used freshly isolated MASMCs. Our results showed that AT1-AAs can directly inhibit the opening capability and calcium sensitivity of BK channel.

Although other studies have shown that angiotensin II can also inhibit BK channels by activating AT_1R, the mechanisms may not be the same. The binding site of angiotensin II on AT_1R is between the second and third extracellular loops of the receptor, while it is located in the second extracellular loop for AT1-AAs.[7] Our studies and others have all found that AT1-AAs can activate AT_1R for a longer period of time than angiotensin II. Specifically, they lead to prolonged activation of AT_1R downstream signals in VSMCs, including Ca^{2+}, protein kinase C, extracellular signal-regulated kinase 1 and 2 and thus cause sustained vasoconstriction.[32,33] Therefore, we speculate that the sustained inhibition of the BK channel by AT1-AAs was due to the sustained activation of AT_1R.

Experiments with HEK293T cells expressing only BK channel α-subunit plasmids indicated the involvement of the α-subunit-dependent mechanism in AT1-AAs-induced BK channel dysfunction. BK channels are channel complexes, composed of a pore-forming and calcium- and voltage-sensing α-subunit, as well as auxiliary β-subunit and γ-subunit. The auxiliary subunits can modify the voltage and calcium dependence of BK channel activation.[34] As reported, BK channel β1-subunit deficiency exacerbates MA fibrosis and remodeling when combined with high fat fed condition.[19] However, evidence to support a role for BK channel α-subunit in vascular remodeling is lacking. *KCNMA1* is the gene that encodes BK channel α-subunit. To elucidate the involvement of BK channel α-subunit in the pathological process of MA remodeling, we used *KCNMA1*$^{-/-}$ rats. As the results showed, MAs from *KCNMA1*$^{-/-}$ rats exhibited similar fibrosis and remodeling as induced by AT1-AAs. Thus, BK channel α-subunit inhibition may explain the vasculopathy observed in AT1-AAs-positive rats.

To test that notion, we used NS1619. NS1619 is a specific BK channel opener and its activating effects are dependent on the α-subunit.[35] NS1619 has been considered to be a potential therapeutic agent in pulmonary hypertension,[36] erectile dysfunction,[37] bladder instability,[38]

shock-induced vascular hyperactivity,[39] migraines,[40] inflammatory pain,[41] neurologic diseases[42] and cytoprotection.[43] Under pathological conditions, injured VSMCs exhibit a phenotypic transformation, from a normal contractile (differentiated) phenotype to a pathological synthetic (dedifferentiated) phenotype. These phenotypically transformed VSMCs proliferate excessively and synthesize a large number of matrix components, which stimulate hypertrophy. Several studies have demonstrated that the BK channel was involved in VSMCs differentiation and proliferation. BK channel openers have been shown to have therapeutic effects in conditions characterized by hyperexcitability and VSMC dysfunction.[44,45] In the present study, AT1-AAs-induced downregulation of contractile proteins and increase in migration were reversed by NS1619 in cultured MASMCs. Therefore, inhibition of BK channel activity activates and primes the phenotypic transition induced by AT1-AAs. To assess the physiological importance of the BK channel in vivo, we used a chronic model of NS1619 infusion. Our results showed that all of the detrimental effects AT1-AAs induced were attenuated by NS1619.

We compared the structures of ZERO-BK α-subunit in humans and rats to identify the homology between them (Figure S13). According to the analysis, the primary structures share a similarity of up to 92.83%. The prediction of the secondary structure shows similar amino acid sites that form α-helices and β-folds (β-sheets or β-strands). Furthermore, the similarity of the 3-level structures is 100%. A decrease in BK channel function has been reported in humans with hypertensive diseases.[46,47] Therefore, it is of practical significance to investigate the inhibitory effects and mechanisms of AT1-AAs on BK channels in human diseases.

CONCLUSIONS

In summary, our study demonstrates that chronic rise in serum AT1-AAs leads to impaired BK channel function and thus causes inward eutrophic MA remodeling. BK channel activation with NS1619 exerts a beneficial effect in MASMC phenotypic transition and MA remodeling by counteracting the stimulus of AT1-AAs. The maladaptive remodeling in the resistance arteries may herald the occurrence of hypertension. Therefore, our findings suggest that strategies for restoring BK channel function may lead to better management of hypertensive vascular diseases and alleviate the associated target-organ damage.

ARTICLE INFORMATION

Received September 21, 2021; Revised November 30, 2021; accepted January 10, 2022.

Affiliations

Department of Physiology and Pathophysiology, School of Basic Medical Sciences, Capital Medical University, Beijing, China (M.W., X.Y., X.Z., M.Y., C.H., X.L., W.W., S.Z., H.L.); Beijing Key Laboratory of Metabolic Disorders Related Cardiovascular Disease, Capital Medical University, Beijing, China (M.W., W.W., S.Z., H.L.); and Division of Adult Cardiac Surgery, Department of Cardiology, The Sixth Medical Center, Chinese PLA General Hospital, Beijing, China (S.L.).

Acknowledgments

We thank Dr. Xiaoqiu Tan from the Key Laboratory of Medical Electrophysiology of the Ministry of Education, Institute of Cardiovascular Research, Southwest Medical University for kindly providing the GFP-ZERO-BK α plasmids.

Sources of Funding

This work was supported by funding from the Natural Sciences Foundation of China (81900415, 31771267) and Beijing Natural Science Foundation Program and Scientific Research Key Program of Beijing Municipal Commission of Education (KZ201810025039).

Disclosures

None.

Supplemental Material

Data S1
Figures S1–S13

REFERENCES

1. Mathiassen ON, Buus NH, Sihm I, Thybo NK, Mørn B, Schroeder AP, Thygesen K, Aalkjaer C, Lederballe O, Mulvany MJ, et al. Small artery structure is an independent predictor of cardiovascular events in essential hypertension. *J Hypertens*. 2007;25:1021–1026. doi: 10.1097/HJH.0b013e32805bf8ed
2. Rizzoni D, Porteri E, Boari GE, De Ciuceis C, Sleiman I, Muiesan ML, Castellano M, Miclini M, Agabiti-Rosei E. Prognostic significance of small-artery structure in hypertension. *Circulation*. 2003;108:2230–2235. doi: 10.1161/01.CIR.0000095031.51492.C5
3. Castorena-Gonzalez JA, Staiculescu MC, Foote C, Martinez-Lemus LA. Mechanisms of the inward remodeling process in resistance vessels: is the actin cytoskeleton involved? *Microcirculation*. 2014;21:219–229. doi: 10.1111/micc.12105
4. Schiffrin EL, Touyz RM. From bedside to bench to bedside: role of renin-angiotensin-aldosterone system in remodeling of resistance arteries in hypertension. *Am J Physiol Heart Circ Physiol*. 2004;287:H435–H446. doi: 10.1152/ajpheart.00262.2004
5. Wei F, Jia X-J, Yu S-Q, Gu Y, Wang L, Guo X-M, Wang M, Zhu F, Cheng X, Wei Y-M, et al. Candesartan versus imidapril in hypertension: a randomised study to assess effects of anti-at1 receptor autoantibodies. *Heart*. 2011;97:479–484. doi: 10.1136/hrt.2009.192104
6. Silverberg D, Younis A, Savion N, Harari G, Yakubovitch D, Sheick Yousif B, Halak M, Grossman E, Schneiderman J. Long-term renin-angiotensin blocking therapy in hypertensive patients with normal aorta may attenuate the formation of abdominal aortic aneurysms. *J Am Soc Hypertens*. 2014;8:571–577. doi: 10.1016/j.jash.2014.04.005
7. Wallukat G, Homuth V, Fischer T, Lindschau C, Horstkamp B, Jüpner A, Baur E, Nissen E, Vetter K, Neichel D, et al. Patients with preeclampsia develop agonistic autoantibodies against the angiotensin at1 receptor. *J Clin Investig*. 1999;103:945–952. doi: 10.1172/JCI4106
8. Wallukat G, Neichel D, Nissen E, Homuth V, Luft FC. Agonistic autoantibodies directed against the angiotensin II AT1 receptor in patients with preeclampsia. *Can J Physiol Pharmacol*. 2003;81:79–83.
9. Yang X, Wang F, Chang H, Zhang S, Yang L, Wang X, Cheng X, Zhang M, Ma XL, Liu H. Autoantibody against AT1 receptor from preeclamptic patients induces vasoconstriction through angiotensin receptor activation. *J Hypertens*. 2008;26:1629–1635. doi: 10.1097/HJH.0b013e328304dbff
10. Velloso EP, Pimentel RL, Braga JF, Cabral AC, Reis ZS, Bader M, Santos RA, Wallukat G. Identification of a novel agonist-like autoantibody in preeclamptic patients. *Am J Hypertens*. 2016;29:405–412.
11. Xia Y, Wen H, Bobst S, Day MC, Kellems RE. Maternal autoantibodies from preeclamptic patients activate angiotensin receptors on human trophoblast cells. *J Soc Gynecol Investig*. 2003;10:82–93. doi: 10.1016/S1071-5576(02)00259-9
12. Wang B, Liao YH, Zhou Z, Li L, Wei F, Wang M, Wei Y. Arterial structural changes in rats immunized by AT1-receptor peptide. *Heart Vessels*. 2005;20:153–158. doi: 10.1007/s00380-005-0825-9

13. Wang M, Yin X, Zhang S, Mao C, Cao N, Yang X, Bian J, Hao W, Fan Q, Liu H. Autoantibodies against at1 receptor contribute to vascular aging and endothelial cell senescence. *Aging Dis* 2019;10:1012–1025. doi: 10.14336/AD.2018.0919
14. Cabral-Marques O, Riemekasten G. Vascular hypothesis revisited: role of stimulating antibodies against angiotensin and endothelin receptors in the pathogenesis of systemic sclerosis. *Autoimmun Rev*. 2016;15:690–694. doi: 10.1016/j.autrev.2016.03.005
15. Sun Y, Li Y, Wang M, Yue M, Bai L, Bian J, Hao W, Sun J, Zhang S, Liu H. Increased AT2R expression is induced by AT1R autoantibody via two axes, Klf-5/IRF-1 and circErbB4/miR-29a-5p, to promote vsmc migration. *Cell Death Dis*. 2020;11:432. doi: 10.1038/s41419-020-2643-5
16. Zhang ZY, Qian LL, Wang RX. Molecular mechanisms underlying renin-angiotensin-aldosterone system mediated regulation of BK channels. *Front Physiol*. 2017;8:698. doi: 10.3389/fphys.2017.00698
17. Hu XQ, Zhang L. Function and regulation of large conductance ca(2+)-activated k+ channel in vascular smooth muscle cells. *Drug Discovery Today*. 2012;17:974–987. doi: 10.1016/j.drudis.2012.04.002
18. Brayden JE, Nelson MT. Regulation of arterial tone by activation of calcium-dependent potassium channels. *Science*. 1992;256:532–535. doi: 10.1126/science.1373909
19. Xu H, Garver H, Fernandes R, Phelps JT, Harkema JJ, Galligan JJ, Fink GD. Bk channel beta1-subunit deficiency exacerbates vascular fibrosis and remodelling but does not promote hypertension in high-fat fed obesity in mice. *J Hypertens*. 2015;33:1611–1623.
20. Wang P, Zhang S, Ren J, Yan L, Bai L, Wang L, Wang P, Bian J, Yin X, Liu H. The inhibitory effect of BKCa channels induced by autoantibodies against angiotensin ii type 1 receptor is independent of AT1R. *Acta Biochim Biophys Sin*. 2018;50:560–566. doi: 10.1093/abbs/gmy038
21. Leo MD, Bulley S, Bannister JP, Kuruvilla KP, Narayanan D, Jaggar JH. Angiotensin ii stimulates internalization and degradation of arterial myocyte plasma membrane BK channels to induce vasoconstriction. *Am J Physiol Cell Physiol*. 2015;309:C392–C402. doi: 10.1152/ajpcell.00127.2015
22. Mathiassen ON, Buus NH, Larsen ML, Mulvany MJ, Christensen KL. Small artery structure adapts to vasodilatation rather than to blood pressure during antihypertensive treatment. *J Hypertens*. 2007;25:1027–1034.
23. Laurent S, Boutouyrie P. The structural factor of hypertension: large and small artery alterations. *Circ Res*. 2015;116:1007–1021. doi: 10.1161/CIRCRESAHA.116.303596
24. Jin Z, Wang J, Zhang W, Zhang G, Jiao X, Zhi J. Changes in cardiac structure and function in rats immunized by angiotensin type 1 receptor peptides. *Acta Biochim Biophys Sin*. 2011;43:970–976. doi: 10.1093/abbs/gmr096
25. Becker NP, Goettel P, Mueller J, Wallukat G, Schimke I. Functional autoantibody diseases: basics and treatment related to cardiomyopathies. *Front Biosci*. 2019;24:48–95. doi: 10.2741/4709
26. Daikha-Dahmane F, Levy-Beff E, Jugie M, Lenclen R. Foetal kidney maldevelopment in maternal use of angiotensin II type I receptor antagonists. *Pediatr Nephrol*. 2006;21:729–732.
27. Boix E, Zapater P, Pico A, Moreno O. Teratogenicity with angiotensin ii receptor antagonists in pregnancy. *J Endocrinol Invest*. 2005;28:1029–1031. doi: 10.1007/BF03345344
28. Rueda A, Fernandez-Velasco M, Benitah JP, Gomez AM. Abnormal ca2+ spark/STOC coupling in cerebral artery smooth muscle cells of obese type 2 diabetic mice. *PLoS One*. 2013;8:e53321. doi: 10.1371/journal.pone.0053321
29. Howitt L, Grayson TH, Morris MJ, Sandow SL, Murphy TV. Dietary obesity increases no and inhibits BKCa-mediated, endothelium-dependent dilation in rat cremaster muscle artery: association with caveolins and caveolae. *Am J Physiol Heart Circ Physiol*. 2012;302:H2464–H2476.
30. Howitt L, Sandow SL, Grayson TH, Ellis ZE, Morris MJ, Murphy TV. Differential effects of diet-induced obesity on BKCa {beta}1-subunit expression and function in rat skeletal muscle arterioles and small cerebral arteries. *Am J Physiol Heart Circ Physiol*. 2011;301:H29–H40.
31. Nystoriak MA, Nieves-Cintron M, Nygren PJ, Hinke SA, Nichols CB, Chen CY, Puglisi JL, Izu LT, Bers DM, Dell'acqua ML, et al. AKAP150 contributes to enhanced vascular tone by facilitating large-conductance ca2+-activated k+ channel remodeling in hyperglycemia and diabetes mellitus. *Circ Res*. 2014;114:607–615. doi: 10.1161/CIRCRESAHA.114.302168
32. Zhang S, Zheng R, Yang L, Zhang XI, Zuo L, Yang X, Bai K, Song LI, Tian J, Yang J, et al. Angiotensin type 1 receptor autoantibody from preeclamptic patients induces human fetoplacental vasoconstriction. *J Cell Physiol*. 2013;228:142–148. doi: 10.1002/jcp.24113
33. Bian J, Lei J, Yin X, Wang P, Wu Y, Yang X, Wang L, Zhang S, Liu H, Fu MLX. Limited AT1 receptor internalization is a novel mechanism underlying sustained vasoconstriction induced by AT1 receptor autoantibody from preeclampsia. *J Am Heart Assoc*. 2019;8:e011179. doi: 10.1161/JAHA.118.011179
34. Dong DL, Bai YL, Cai BZ. Calcium-activated potassium channels: potential target for cardiovascular diseases. *Adv Protein Chem Struct Biol*. 2016;104:233–261.
35. Latorre R, Castillo K, Carrasquel-Ursulaez W, Sepulveda RV, Gonzalez-Nilo F, Gonzalez C, Alvarez O. Molecular determinants of BK channel functional diversity and functioning. *Physiol Rev*. 2017;97:39–87. doi: 10.1152/physrev.00001.2016
36. Vang A, Mazer J, Casserly B, Choudhary G. Activation of endothelial BKCa channels causes pulmonary vasodilation. *Vascul Pharmacol*. 2010;53:122–129. doi: 10.1016/j.vph.2010.05.001
37. Gonzalez-Corrochano R, La Fuente J, Cuevas P, Fernandez A, Chen M, Saenz de Tejada I, Angulo J. Ca2+ -activated k+ channel (KCa) stimulation improves relaxant capacity of PDE5 inhibitors in human penile arteries and recovers the reduced efficacy of PDE5 inhibition in diabetic erectile dysfunction. *Br J Pharmacol*. 2013;169:449–461.
38. La Fuente JM, Fernandez A, Cuevas P, Gonzalez-Corrochano R, Chen MX, Angulo J. Stimulation of large-conductance calcium-activated potassium channels inhibits neurogenic contraction of human bladder from patients with urinary symptoms and reverses acetic acid-induced bladder hyperactivity in rats. *Eur J Pharmacol*. 2014;735:68–76. doi: 10.1016/j.ejphar.2014.03.060
39. Hu Y, Yang G, Xiao X, Liu L, Li T. BKCa opener, NS1619 pretreatment protects against shock-induced vascular hyporeactivity through PDZ-rho GEF-RhoA-rho kinase pathway in rats. *J Trauma Acute Care Surg*. 2014;76:394–401. doi: 10.1097/TA.0b013e3182aa2d98
40. Lu R, Lukowski R, Sausbier M, Zhang DD, Sisignano M, Schuh CD, Kuner R, Ruth P, Geisslinger G, Schmidtko A. BKCa channels expressed in sensory neurons modulate inflammatory pain in mice. *Pain*. 2014;155:556–565. doi: 10.1016/j.pain.2013.12.005
41. Akerman S, Holland PR, Lasalandra MP, Goadsby PJ. Inhibition of trigeminovascular dural nociceptive afferents by Ca(2+)-activated K(+) (MaxiK/BK(Ca)) channel opening. *Pain*. 2010;151:128–136. doi: 10.1016/j.pain.2010.06.028
42. Gaspar T, Domoki F, Lenti L, Katakam PV, Snipes JA, Bari F, Busija DW. Immediate neuronal preconditioning by ns1619. *Brain Res*. 2009;1285:196–207. doi: 10.1016/j.brainres.2009.06.008
43. Xu W, Liu Y, Wang S, McDonald T, Van Eyk JE, Sidor A, O'Rourke B. Cytoprotective role of ca2+- activated k+ channels in the cardiac inner mitochondrial membrane. *Science*. 2002;298:1029–1033.
44. Wan XJ, Zhao HC, Zhang P, Huo B, Shen BR, Yan ZQ, Qi YX, Jiang ZL. Involvement of BK channel in differentiation of vascular smooth muscle cells induced by mechanical stretch. *Int J Biochem Cell Biol*. 2015;59:21–29. doi: 10.1016/j.biocel.2014.11.011
45. Jia X, Yang J, Song W, Li P, Wang X, Guan C, Yang L, Huang Y, Gong X, Liu M, et al. Involvement of large conductance Ca(2+)-activated K(+) channel in laminar shear stress-induced inhibition of vascular smooth muscle cell proliferation. *Pflugers Arch*. 2013;465:221–232. doi: 10.1007/s00424-012-1182-z
46. Yang Y, Li PY, Cheng J, Mao L, Wen J, Tan XQ, Liu ZF, Zeng XR. Function of BKCa channels is reduced in human vascular smooth muscle cells from Han Chinese patients with hypertension. *Hypertension*. 2013;61:519–525. doi: 10.1161/HYPERTENSIONAHA.111.00211
47. Amberg GC, Bonev AD, Rossow CF, Nelson MT, Santana LF. Modulation of the molecular composition of large conductance, Ca(2+) activated K(+) channels in vascular smooth muscle during hypertension. *J Clin Investig*. 2003;112:717–724. doi: 10.1172/JCI200318684

SUPPLEMENTAL MATERIAL

Data S1.

Supplemental Materials and Methods

Animal experiments

All experimental procedures were approved by the Institutional Animal Care and Use Committee and Ethics Committee of Capital Medical University (Beijing, China) and were in strict accordance with the recommendation in the Guide for the Care and Use of Laboratory Animals of the National Institutes of Health. Healthy male Sprague-Dawley (SD) rats aged 8 weeks (140-160 g) were obtained from the Animal Center of Capital Medical University and housed under a 12:12-h dark-light cycle in standard conditions of humidity and room temperature. Before immunization, blood collection from the tip of the tail, or the subcutaneous implantation of osmotic mini-pumps, rats were anaesthetized with an intraperitoneal injection of 40 mg/kg sodium pentobarbital. At the end of the experiment, the rats were euthanized with an intraperitoneal injection of 100 mg/kg sodium pentobarbital. Active immunization was carried out as previously described[14]. Briefly, male SD rats aged 8 weeks were randomly divided into two groups: the Freund's adjuvant emulsified AT_1R-ECII peptide-immunized group and the Freund's adjuvant emulsified saline-treated vehicle group. The immunization was repeated by subcutaneous injection with AT_1R-ECII every two weeks. The blood pressure was measured at 2-week intervals with the standard tail-cuff technique (Softron, Japan) using the Powerlab system. Blood samples were collected every two weeks before immunization. The relative amounts of AT1-AAs in sera were determined by enzyme-linked immunosorbent assay (ELISA) as previously described[14]. The preparation of immunoglobulin G from serum was performed as previously described[14]. For the *in vivo* experiments involving NS1619 treatment, saline-treated or peptide fragments-immunized rats were divided into four groups at the end of the 4th week of immunization. Rats were infused with NS1619 (20 μg/kg per day) for 6 weeks via implanted osmotic mini-pumps. $AT1R^{-/-}$ and *KCNMA1*$^{-/-}$ rats were constructed by Nanjing Biomedical Research Institute of Nanjing University.

Materials

The synthetic peptides corresponding to the sequence of the second extracellular loop of human AT_1R (AT_1R-ECII, residues 165-191, sequence I-H-R-N-V-F-F-I-E-N-T-N-I-T-V-C-A-F-H-Y-E-S-Q-N-S-T-L, 95% purity) were purchased form GL Biochem Ltd, Shanghai. Angiotensin II was purchased from Sigma-Aldrich (St. Louis, MO, USA). NS1619 was purchased from Abcam (Cambridge, UK) and dissolved in DMSO (Sigma-Aldrich) as stock solution. Antibodies against α-SMA, Calponin, MYH11 and eIF5 were purchased from Abcam (Cambridge, UK). GFP-ZERO-BK α-subunit plasmids were kindly provided by Dr. Xiaoqiu Tan (Key Laboratory of Medical Electrophysiology of the Ministry of Education, Southwest Medical University).

Histological analysis of vascular morphology

After rats were perfusion-fixed with 4% neutrally buffered paraformaldehyde, the third-order branches of the MAs were excised and embedded in paraffin. The tissues were cut into 5-μm cross

sections and subjected to hematoxylin-eosin and Masson's trichrome staining. The media wall thickness and inner/external lumen diameters of the MAs were measured with a microscope (Olympus, Japan) and image analysis system. Media cross-sectional area (CSA) was calculated as $(\pi/4)$ x $(D_e^2-D_i^2)$, where D_e and D_i are external and lumen diameters, respectively.

Verification of the splicing variants of BK α

Total RNA was extracted from MAs of normal SD rats and then equal amounts (2 μg) were reverse-transcribed into cDNA. The cDNA was amplified by polymerase chain reaction (PCR) using the constructed BK-trans primers. After that, the amplified products were subjected to electrophoretic analysis.

Acute isolation of rat MASMCs

Freshly isolated second- and third-order branches of MAs without perivascular adipose tissues were cut into 2-3 mm pieces in ice-cold oxygenated Tyrode's solution: 127 mM NaCl, 5.9 mM KCl, 1.2 mM $MgCl_2 \cdot 6H_2O$, 10 mM HEPES, and 15 mM glucose. The pH was adjusted to 7.4 using NaOH. Pieces were incubated in Tyrode's solution that contained papain (0.5 mg/mL), DTT (1 mg/mL), and BSA (1 mg/mL) in a water bath at 37 ℃ for 4 min. The arterial vessels were further digested with collagenase II (1 mg/mL)/Tyrode's solution in a water bath at 37℃ for 9 min until the tissue was observed to be loose under the microscope. The enzyme solution was discarded carefully, and Tyrode's solution was slowly added along the tube wall to dilute the enzyme to stop the reaction. The tube was shaken gently, and the solution was carefully discarded; 1ml of Tyrode's solution was then added. Under a microscope, the earthworm-like MASMCs were visible in the suspension. After the cells had attached to the bottom of the dish, they can be used for the patch clamp experiment.

Patch clamp experiment

The single-channel recording was performed at room temperature (22-24℃) using the voltage-clamp technique in a cell-attached (on-cell) and inside-out configuration. The single-channel currents of BK channels were monitored using pCLAMP9.2 software (Molecular Devices). Patch pipettes (Sutter, Novato, USA) and Narishige Model PB-7 micropipette pullers (Narishige, Japan) were used. The cell-attached patch: pipette resistances were ~4-6 MΩ when filled with pipette solution: 40 mM K-ASP, 100 mM KCl, 10 mM HEPES. The pH was adjusted to 7.4 using KOH. The extracellular (bath) solution contained 100 mM K-ASP, 40 mM KCl, 10 mM glucose, 10 mM HEPES, and 1 mM EGTA. The pH was adjusted to 7.4 using KOH. The solutions described above were the same for both the cell-attached and inside-out patches. The holding potential was 0 mV; test pulses were from 0 to +100 mV. The Boltzmann equation was used for the fitting and standardization: $NP_o = NP_{o\ max} / (1 + \exp [(P_{50}-P)/k])$. Exponential distribution function in logarithmic form was used to fit the continuously changing average opening time of BK channels. The inside-out patch: after recording the electrical activity of the BK channel with the cell-attached patch, the membrane was lifted slightly to separate from the cell, thus forming the inside-out patch.

Cell experiments

MASMCs were isolated from the MAs of male SD rats using the enzymatic digestion method.

Briefly, the second to fourth branches of MAs were harvested and removed of the connective tissues in the adventitia. Then the arteries were cut into small pieces and digested with 1 mg/ml trypsin at 37 ℃ for 10 min. After centrifugation, the precipitate was resuspended with 1 mg/ml collagenase type I for about 2 h. Following centrifugation, MASMCs were seeded in DMEM supplemented with 10% fetal bovine serum (HyClone) at 37℃ in a 5% CO_2 atmosphere. The cell cultures contained >95% VSMCs as determined by α-SMA staining. MASMCs from passages 3~8 were used for the experiments. To evaluate the effects of AT1-AAs, MASMCs at 80~90% confluence were incubated with NS1619 (4 μM) for 30 min and then stimulated with 0.1 μM AT1-AAs for 48 hours. The total proteins were used to assess the phenotypic transition induced by AT1-AAs.

MASMC migration assay

MASMC migration was assessed by scratch-wound assay. MASMCs were seeded with the same numbers in six-well plates with indicated stimulations. Scratch wounds were created using pipette tips when the cells grew to 95 confluence. Four fields were randomly selected in each well to record gap distances following scratching at 24 hours to calculate cell migration.

Plasmids transfection

The full-length ZERO-BK α-subunit coding sequence was subcloned into a C-terminal GFP pcDNA3.1 vector. HEK293T cells were transfected using Lipofectamine 3000 Transfection Reagent (Invitrogen, Carlsbad, USA) by following the manufacturer’s instructions. Transfected cells were incubated at 37℃ for an additional 48 hours and then subjected to patch-clamp experiments.

Supplemental Figure Legends:

Figure S1. Assessments of rats in the control and immunized groups.
(A) The serum levels of AT1-AAs in rats of the control and immunized groups. High levels of AT1-AAs were detected in rats immunized with the synthetic AT_1R-EC_{II}. ELISA was used for the detection. Heart rate (**B**), SBP (**C**) and DBP (**D**) curves of rats from the control and immunized groups. Data were analyzed by two-way ANOVA followed by the Bonferroni post hoc test. n = 6-8 rats per group. **P*<0.05, ***P*<0.01, ****P*<0.001, *****P*<0.0001. OD, optical density; AT_1R-EC_{II}, epitope peptide of the extracellular second loop of the AT_1R.

Figure S2. Identification of the types of the splicing variants of the BK channel α-subunit in rat MAs.
Total RNA of MAs from normal SD rats was extracted and reverse-transcribed. **(A)** Schematic diagram of BK-trans primers used for PCR amplification. **(B)** The electrophoresis image for the amplified products showing two bands, of which the 230 bp band corresponded to ZERO-BK α-subunit and the 400 bp band corresponded to STREX-BK α-subunit (n = 6). MAs, mesenteric arteries.

Figure S3. Detection of BK channel protein in the control and immunized groups.
Representative images and statistical diagrams of BK α expression. The data were presented as the means ±SEM (n=3). ns, not significant.

Figure S4. Detection of the purity and biological activity of the extracted AT1-AAs.
(A) Coomassie blue staining showed that IgGs purified from the AT1-AAs-positive rat sera had high purity, which manifested as strong heavy and light chains with sizes of 55 kDa and 25 kDa, respectively. **(B)** Increases in the beating numbers of NRCMs with or without purified AT1-AAs treatment (n = 6). Data were analyzed by Student's *t* test. ***P* < 0.01.

Figure S5. Detection of BK channel function in MASMCs from $AT_1R^{-/-}$ rats.
A, The electrical activity of the BK channel was recorded in MASMCs isolated from $AT_1R^{-/-}$ rats. **B**, The opening probability of the BK channel with increasing voltage stimulation. Data are expressed as the means ±SEM,n= 4 rats per group.

Figure S6. Detection of BK channel function in MASMCs in response to Ang II or AT1-AAs.
The opening probability of BK channels in MASMCs treated with Ang II (0.1 μM) or AT1-AAs (0.1 μM) for the indicated times (n = 4). ***P*<0.01, ns, not significant.

Figure S7. Successful transfection of GFP-ZERO-BK α-subunit plasmids in HEK293T cells.
(A) HEK293T cells successfully transfected with GFP-ZERO-BK α-subunit plasmids expressing green fluorescence. **(B)** Recording of the electrical activity of BK channels in cells successfully transfected with GFP-ZERO-BK α-subunit plasmids or not.

Figure S8. Construction and assessments of the *KCNMA1*$^{-/-}$ rats.
(A) Schematic diagram of the genomic deletion of *KCNMA1*. **(B)** Genomic PCR results of the

KCNMA1$^{-/-}$ rats. Heart rate (**C**), SBP (**D**) and DBP (**E**) curves of rats from the wild type and *KCNMA1*$^{-/-}$ groups. Data were analyzed by Student's *t* test. n = 7 or 8 rats per group. ***P*<0.01, ns, not significant.

Figure S9. Detection of the BK channel activity.
The opening probability of the BK channel with increasing voltage stimulation in MASMCs with or without NS1619 (4 μM) plus AT1-AAs (0.1 μM) treatment (n = 4).

Figure S10. Assessment of the purity of the isolated MASMCs.
The cultured MASMCs were stained with α-SMA. The cell cultures contained >95% VSMCs as determined by α-SMA staining.

Figure S11. Detection of BK channel protein in response to NS1619.
(A) Representative images and statistical diagrams of BK α expression. MASMCs were treated with NS1619 (4 μM) for 48 hours. Cell lysates were prepared and subjected to Western blotting analysis. The data were from 3 independent experiments and presented as the means ±SEM. ns, not significant.

Figure S12. Assessments of the systolic blood pressure of rats in the control and immunized groups with or without NS1619 perfusion.
SBP of rats from the control and immunized groups with or without NS1619 treatment. n = 6-8 rats per group. ns, not significant.

Figure S13. Homology comparison analysis of BK proteins between humans and rats.
(A) Homology comparison of the primary structures of ZERO-BK α-subunit protein between humans and rats. Prediction of physical and chemical properties based on amino acid sequences showed great similarity. **(B)** Homology comparison of the secondary structures of ZERO-BK α-subunit protein between humans and rats. According to the amino acid sequences, the possible sites of α-helices and β-folds and the structures that may be exposed or hidden inside and outside of the protein conformation are predicted. **(C)** Simulated three-dimensional structures of BK channel protein based on amino acid sequences.

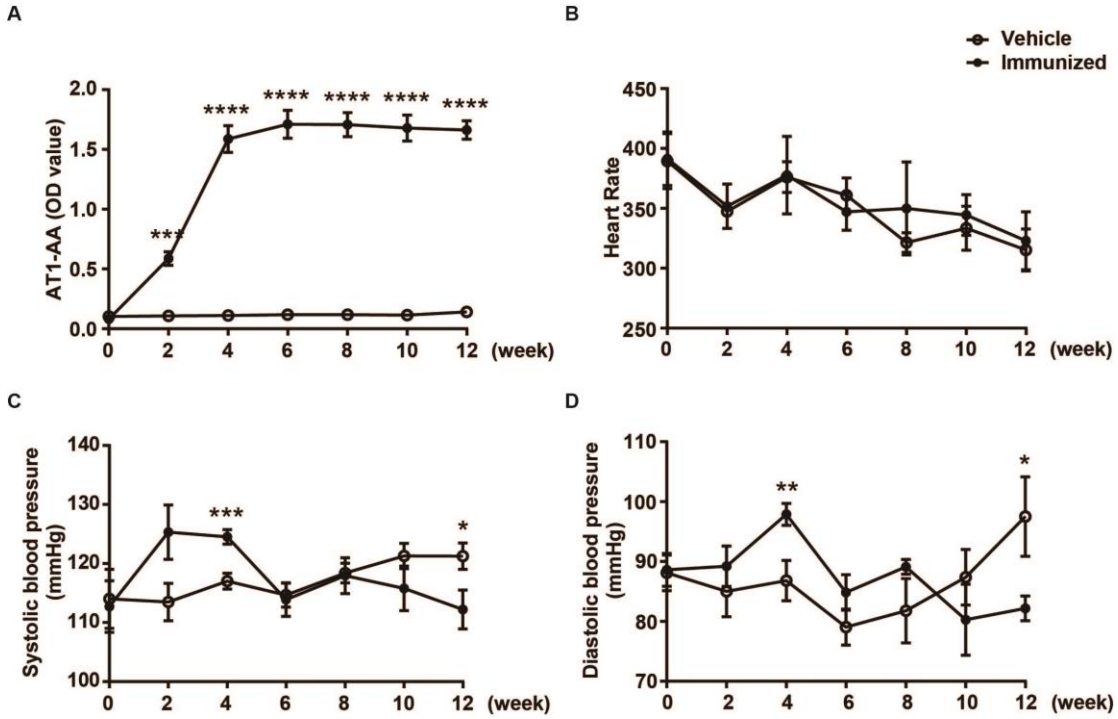

Figure S1. Assessments of rats in the control and immunized groups.

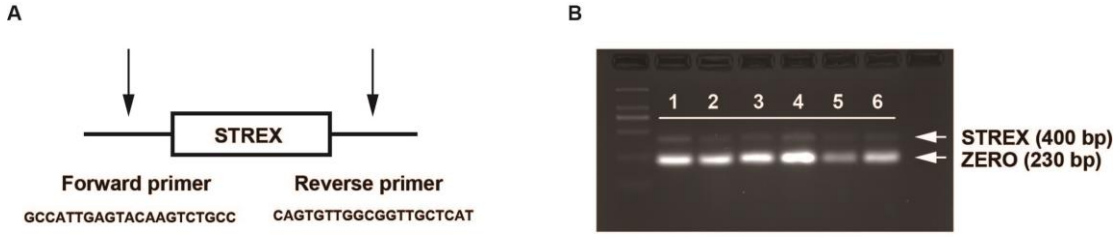

Figure S2. Identification of the types of the splicing variants of the BK channel α-subunit in rat MAs.

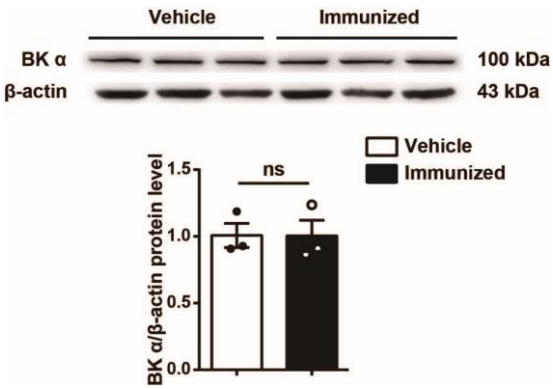

Figure S3. Detection of BK channel protein in the control and immunized groups.

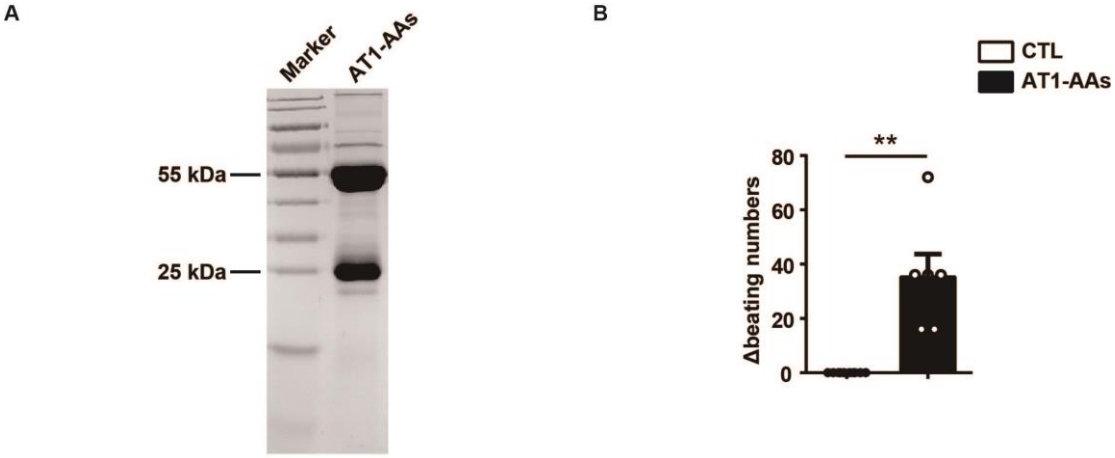

Figure S4. Detection of the purity and biological activity of the extracted AT1-AAs.

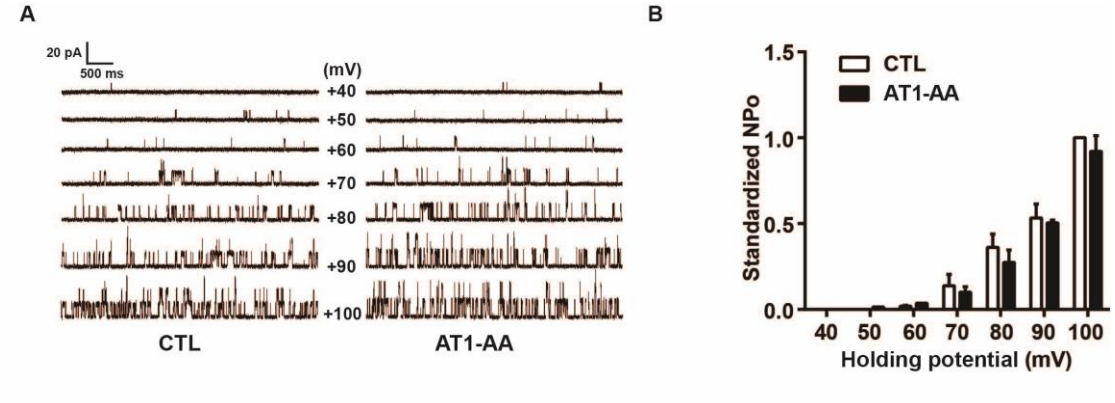

Figure S5. Detection of BK channel function in MASMCs from $AT_1R^{-/-}$ rats.

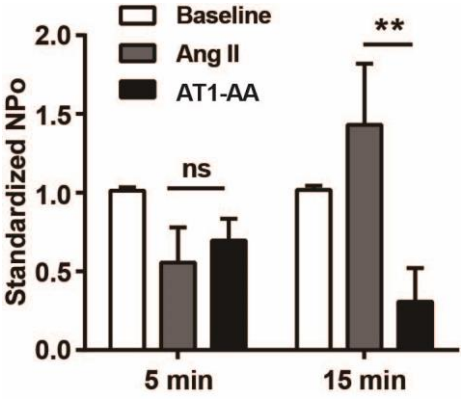

Figure S6. Detection of BK channel function in MASMCs in response to Ang II or AT1-AAs.

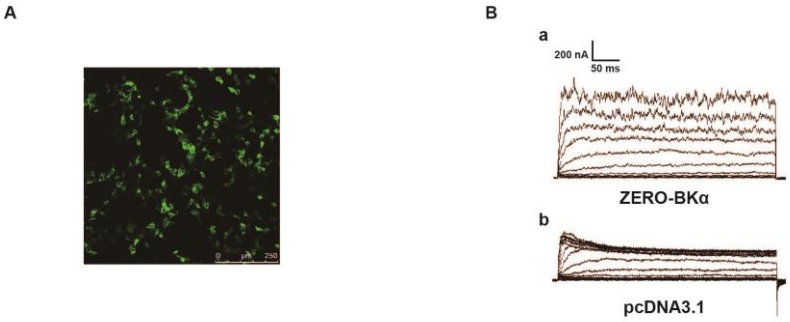

Figure S7. Successful transfection of GFP-ZERO-BK α-subunit plasmids in HEK293T cells.

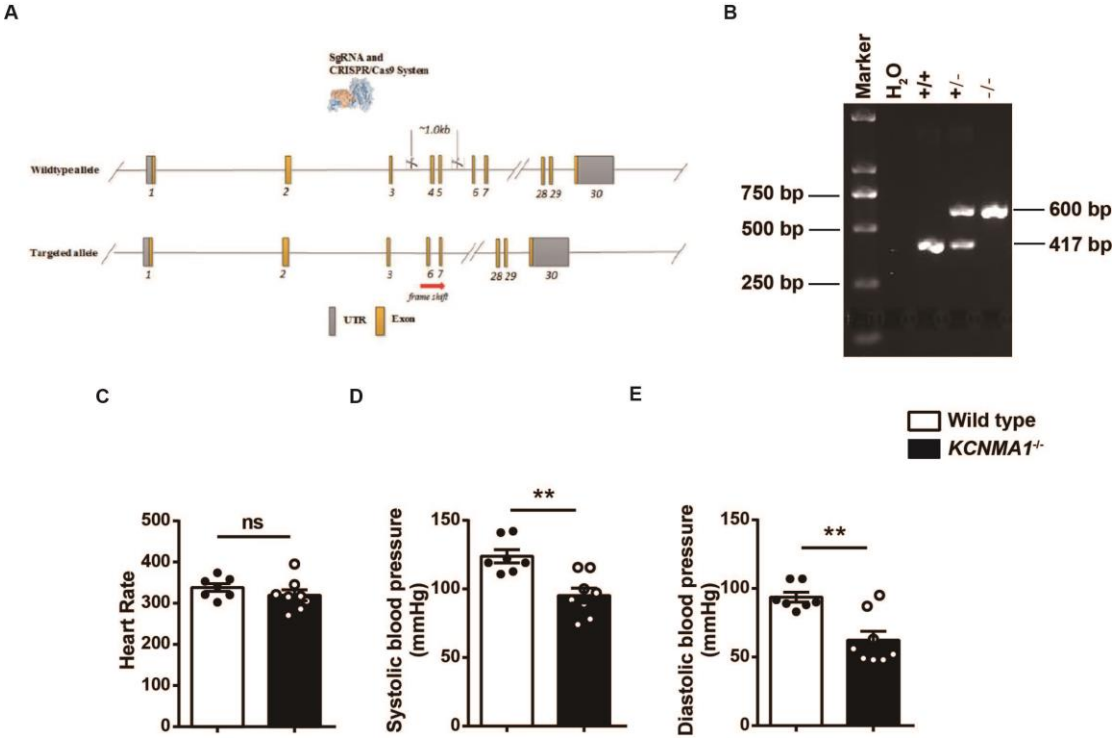

Figure S8. Construction and assessments of the *KCNMA1*$^{-/-}$ rats.

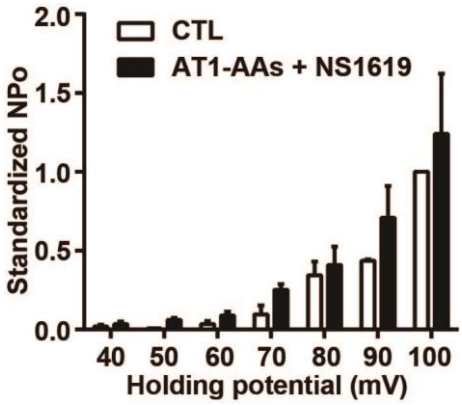

Figure S9. Detection of the BK channel activity.

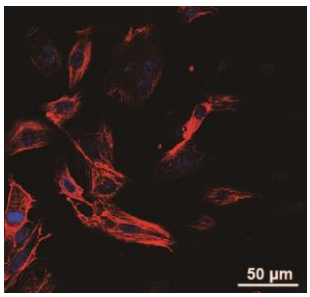

Figure S10. Assessment of the purity of the isolated MASMCs.

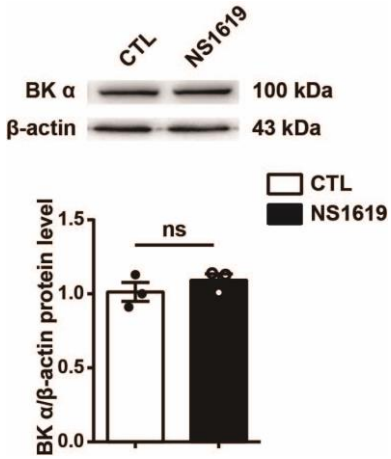

Figure S11. Detection of BK channel protein in response to NS1619.

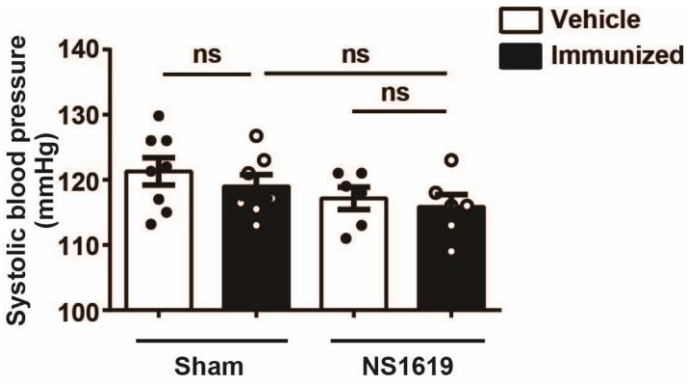

Figure S12. Assessments of the systolic blood pressure of rats in the control and immunized groups with or without NS1619 perfusion.

A

	Homo sapiens	Rattus norvegicus
Align indent. (%)	100	92.83
Number of amino acids	1236	1209
Theoretical pI	6.66	6.68
Estimated half-life (hrs)	30	30
Instability index	52.01	49.96
Aliphatic index	88.35	90.80
Grand average of hydropathicity	-0.075	-0.064

B

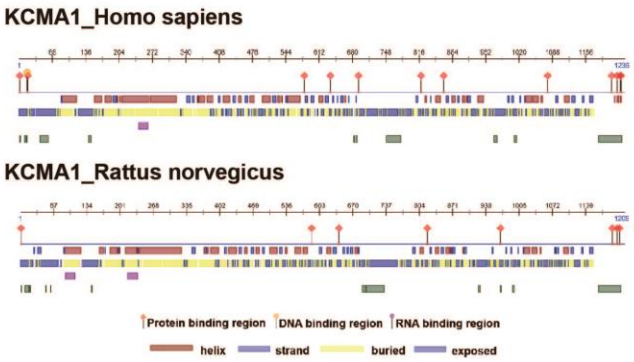

C

Figure S13. Homology comparison analysis of BK proteins between humans and rats.